

# Lawrence Berkeley National Laboratory

## LBL Publications

### Title

Cooperative Carbon Dioxide Adsorption in Alcoholamine- and Alkoxyalkylamine-Functionalized Metal-Organic Frameworks.

### Permalink

<https://escholarship.org/uc/item/3kj396d4>

### Authors

Mao, VY  
Milner, PJ  
Lee, J-H  
[et al.](#)

### Publication Date

2019-12-26

### DOI

10.1002/anie.201915561

Peer reviewed

# Cooperative Carbon Dioxide Capture in Alcoholamine- and Alkoxyalkylamine-Functionalized Metal–Organic Frameworks

Victor Y. Mao, Phillip J. Milner, Jung-Hoon Lee, Alexander C. Forse, Eugene Kim, Rebecca L. Siegelman, C. Michael McGuirk, Leo B. Porter-Zasada, Jeffrey B. Neaton, Jeffrey A. Reimer, and Jeffrey R. Long<sup>[a]</sup>

**Abstract:** A series of structurally diverse alcoholamine- and alkoxyalkylamine-functionalized variants of the metal–organic framework  $\text{Mg}_2(\text{dobpdc})$  are shown to exhibit selective, step-shaped adsorption of carbon dioxide ( $\text{CO}_2$ ). Optimized structures obtained from vdW-corrected DFT calculations indicate that the observed adsorption profiles can be attributed to carbamic acid (for alcoholamines) or ammonium carbamate (for alkoxyalkylamines) chain-like structures stabilized by hydrogen bonding interactions within the framework pores, as corroborated by solid state NMR. As the first report of materials exhibiting cooperative  $\text{CO}_2$  chemisorption without the use of diamines, this finding provides the foundation for expanding the scope of cooperative  $\text{CO}_2$  capture in porous materials.

## I. Introduction

It has been well-documented that recent atmospheric carbon dioxide ( $\text{CO}_2$ ) levels have been rising rapidly, with  $\text{CO}_2$

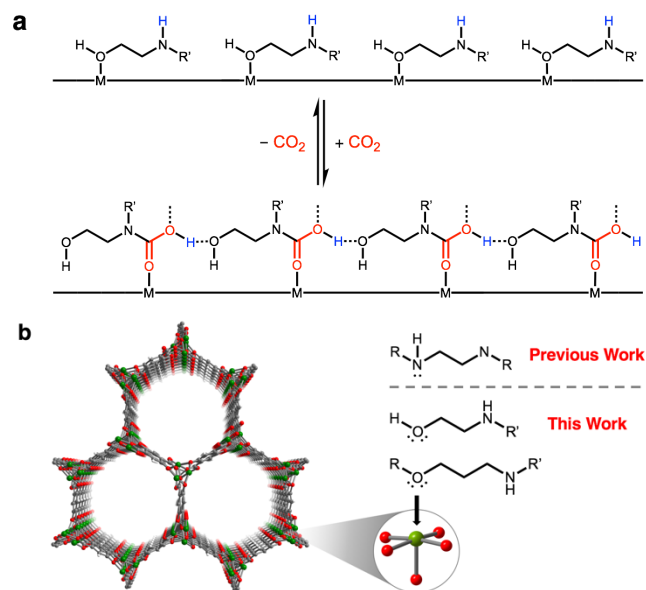


**Figure 1.** a) Proposed  $\text{CO}_2$  adsorption mechanism for alcoholamine-appended  $\text{Mg}_2(\text{dobpdc})$  involving hydrogen bond-stabilized carbamic acid chains. b) Representative structure of the metal–organic framework  $\text{Mg}_2(\text{dobpdc})$ . The inset shows a single open  $\text{Mg}^{2+}$  site appended with an alcoholamine or alkoxyalkylamine. Grey, red, and green spheres represent C, O, and Mg atoms, respectively; H atoms are omitted for clarity.

levels exceeding an unprecedented average of 400 ppm globally in 2016.<sup>1</sup> Studies have shown that the continued rise of  $\text{CO}_2$  atmospheric levels will likely have irreversible impacts on the planet's climate.<sup>5</sup> To date, fossil fuel combustion accounts for the largest percentage of anthropogenic  $\text{CO}_2$  emissions,<sup>2</sup> and as such, the development of cost-effective strategies for mitigating  $\text{CO}_2$  emissions from traditional energy sources is paramount. A proposed strategy to reduce anthropogenic  $\text{CO}_2$  emissions from point sources is carbon capture and sequestration (CCS).<sup>1</sup> The implementation of CCS using current technologies would be expensive, however, leading to an estimated >30% increase in the levelized cost of electricity.<sup>3,4</sup> Because the  $\text{CO}_2$  capture step represents approximately 70–80% of the cost associated with CCS,<sup>3</sup> the development of new carbon capture materials could dramatically increase the cost-efficiency and applicability of CCS.

Recently, it has been shown that diamine-appended variants of  $\text{Mg}_2(\text{dobpdc})$  ( $\text{dobpdc}^{4-} = 4,4'$ -dioxidobiphenyl-3,3'-dicarboxylate), a metal–organic framework with coordinatively unsaturated  $\text{Mg}^{2+}$  sites, capture  $\text{CO}_2$  through a unique cooperative adsorption mechanism involving the insertion of  $\text{CO}_2$  into  $\text{Mg}-\text{N}$  bonds to form ammonium carbamate chains (Figure 1).<sup>7</sup> This mechanism allows for selective capture of  $\text{CO}_2$  and results in step-shaped adsorption profiles, which in turn enable high working capacities with low regeneration energies.

[a] V. Y. Mao, Dr. A. C. Forse, Prof. J. A. Reimer, Prof. J. R. Long  
Department of Chemical and Biomolecular Engineering  
The University of California, Berkeley  
Berkeley CA, 94720 (USA)  
E-mail: victor.mao@berkeley.edu

Dr. A. C. Forse, E. Kim, R. L. Siegelman, Dr. C. M. McGuirk, Prof. J. R. Long  
Department of Chemistry  
The University of California, Berkeley  
Berkeley CA, 94720 (USA)

Dr. J. Lee, Prof. J. B. Neaton  
Department of Physics  
The University of California, Berkeley  
Berkeley CA, 94720 (USA)

Prof. P. J. Milner  
Department of Chemistry and Chemical Biology  
Cornell University  
Ithaca NY, 14850 (USA)

R. L. Siegelman  
Materials Sciences Division  
Lawrence Berkeley National Laboratory  
Berkeley CA, 94720 (USA)

Dr. A. C. Forse  
Berkeley Energy and Climate Institute  
The University of California, Berkeley  
Berkeley CA, 94720 (USA)

Dr. J. Lee, Prof. J. B. Neaton  
The Molecular Foundry  
Lawrence Berkeley National Laboratory  
1 Cyclotron Rd., Berkeley CA, 94720 (USA)

Dr. J. Lee, Prof. J. B. Neaton  
The Kavli Energy Nanosciences Institute  
The University of California, Berkeley  
Berkeley CA, 94720 (USA)

Furthermore, these materials can be structurally tuned to fit the required operating conditions for a given process, making them leading candidates for carbon capture applications.<sup>9,10</sup> However, ammonium carbamate chain formation remains the only cooperative CO<sub>2</sub> chemisorption mechanism known to date, which greatly restricts the library of usable materials.

We have recently shown that changing the structure of the diamine in these materials can lead to new adsorption mechanisms, such as the formation of carbamic acid pairs.<sup>9</sup> Based on this finding, we envisioned that more significant variations in this system, including changing the appended diamines to other bifunctional molecules such as alcoholamines (Figure 1), could not only reveal new mechanisms for cooperative adsorption but also greatly expand the range of materials suitable for carbon capture applications. Herein, we demonstrate via a combination of gas sorption, spectroscopic, and computational studies that alcoholamine- and alkoxyalkylamine-appended variants of Mg<sub>2</sub>(dobpdc) are also capable of undergoing cooperative CO<sub>2</sub> adsorption through related but distinct mechanisms.

## II. Results and Discussion

### Step-shaped CO<sub>2</sub> Adsorption in Alcoholamine-Appended Mg<sub>2</sub>(dobpdc) Variants

Alcoholamines are attractive functionalities in the design of new scalable adsorbents for carbon capture, as they are typically significantly less expensive than the corresponding diamines. Indeed, current large-scale carbon capture applications are

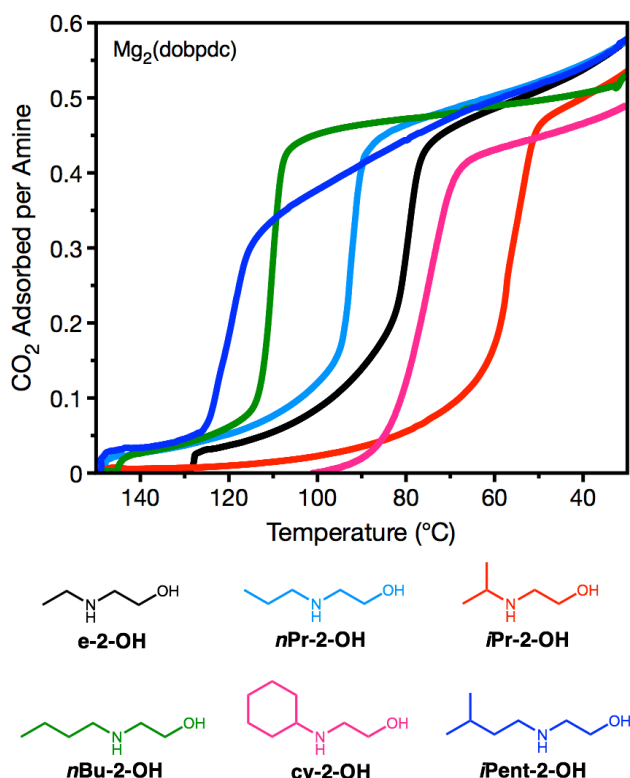


**Figure 2.** Pure CO<sub>2</sub> adsorption isobars at atmospheric pressure for e-2-OH-, nPr-2-OH-, iPr-2-OH-, nBu-2-OH-, cy-2-OH-, and iPent-2-OH-Mg<sub>2</sub>(dobpdc), as measured by thermogravimetric analysis. Each framework exhibits a maximum capacity of 0.5 CO<sub>2</sub> per amine, or 1 CO<sub>2</sub> per two alcoholamines.

primarily carried out with aqueous alcoholamine solutions due to their low cost and scalability.<sup>15</sup> However, the previously reported cooperative adsorption of CO<sub>2</sub> is facilitated by the ability of diamines to form extended chains in which one amine has reacted with CO<sub>2</sub> and the other has accepted a proton to form an ammonium species.<sup>7</sup> Because alcoholamines cannot react by this mechanism,<sup>14</sup> it was unclear prior to this work if alcoholamine-appended frameworks could undergo cooperative adsorption via

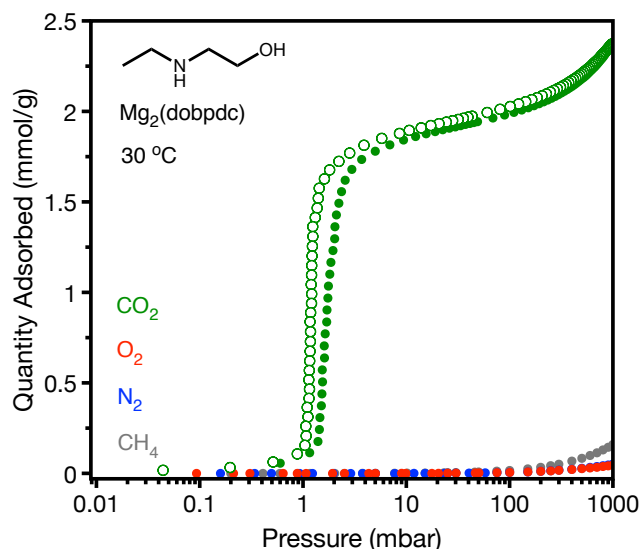


**Figure 3.** Single-component isotherms for e-2-OH-Mg<sub>2</sub>(dobpdc). Closed circles indicate adsorption, and open circles indicate desorption. A capacity of 2 mmol/g corresponds to 1 CO<sub>2</sub> adsorbed per 2 molecules of e-2-OH.

a different mechanism.

In order to probe the CO<sub>2</sub> adsorption properties of alcoholamine-appended frameworks, a diverse range of alcoholamines were grafted to the parent framework Mg<sub>2</sub>(dobpdc) using our previously reported procedure.<sup>7</sup> Gratifyingly, reversible step-shaped adsorption was found to occur with alcoholamines bearing moderately bulky secondary amines. Namely, the ethyl (e-2-OH), *n*-propyl (nPr-2-OH), isopropyl (iPr-2-OH), *n*-butyl (nBu-2-OH), cyclohexyl (cy-2-OH), and isoamyl (iPent-2-OH) substituents distinctly display this behavior in both isobaric (Figure 2) and isothermal (Figure S198, S199) measurements. Other alcoholamines, such as 3-aminopropanol (3-OH), exhibited modest cooperative adsorption as well (SI, Section 8). As expected, minimal, non-cooperative adsorption was observed with O<sub>2</sub>, N<sub>2</sub>, and CH<sub>4</sub>, other gases relevant to CO<sub>2</sub> capture applications (Figure 3). Because the alcoholamines in these materials cannot react with CO<sub>2</sub> to form ammonium carbamate chains, they must operate by a new cooperative chemisorption mechanism (see below). Indeed, while the differential enthalpy of CO<sub>2</sub> adsorption in e-2-OH-Mg<sub>2</sub>(dobpdc) is comparable to that previously reported<sup>10</sup> for the corresponding diamine-appended framework e-2-Mg<sub>2</sub>(dobpdc) (−81 ± 4 vs. −84 ± 3 kJ/mol, respectively), the entropic penalty is much larger (−214 ± 11 vs. −186 ± 14 J/mol·K, respectively) (Figure S203), which is consistent with a different mechanism for cooperative adsorption.<sup>9</sup>

Increasing the amine substituent size with alcoholamines generally decreased the adsorption threshold, thereby increasing the isobaric step temperature (equivalent to a lower step pressure

in an isotherm).<sup>10</sup> For example, under pure CO<sub>2</sub>, the adsorption step temperatures range from 60 °C (*i*Pr-2-OH) to 125 °C (*i*Pent-2-OH), with larger and longer amine substituents generally shifting the adsorption step to higher temperatures (Figure 2). Isothermal measurements reflected identical trends in the favorability of CO<sub>2</sub> adsorption in these materials (SI, Section 21). Notably, alcoholamine-appended Mg<sub>2</sub>(dobpdc) variants with very sterically hindered amine substituents (e.g. *t*-Butyl), as well as those with tertiary amines, did not appreciably adsorb CO<sub>2</sub>, suggesting that reaction at the amine sites is key to the adsorption mechanism (SI, Section 8).

For the series of 2-(alkylamino)ethanol-appended frameworks that do exhibit step-shaped adsorption, the observed post-step adsorption capacity corresponds to 1 CO<sub>2</sub> molecule per two alcoholamines. While this capacity is half that corresponding to 1 CO<sub>2</sub> per diamine we had observed previously in diamine-appended variants of Mg<sub>2</sub>(dobpdc), it does maintain the adsorption ratio of 1 CO<sub>2</sub> per two amines.<sup>7</sup> Double-step adsorption behavior has been previously reported for diamine-appended variants of Mg<sub>2</sub>(dobpdc) with bulky substituents due to steric interactions between adjacent diamines in the *a-b* plane of the framework.<sup>8</sup> However, unlike in our previous work, cooling e-2-OH-Mg<sub>2</sub>(dobpdc) under pure CO<sub>2</sub> in a differential scanning calorimeter to -70 °C did not reveal the presence of a second adsorption step below the primary adsorption step at 80 °C (Figure S173). This suggests that the “half capacity” observed in alcoholamine-appended frameworks is likely not due to the steric interactions and cannot be overcome by increasing the driving force for CO<sub>2</sub> adsorption. In addition, appending the same alcoholamines to frameworks with a larger spacing between metal sites in the *a-b* plane, namely Mg<sub>2</sub>(pc-dobpdc) (pc-dobpdc<sup>4-</sup> = 3,3'-dihydroxy-[1,1'-biphenyl]-4,4'-dicarboxylic acid) and Mg<sub>2</sub>(dotpdc) (dotpdc<sup>4-</sup> = 4,4'-dioxido-[1,1':4',1''-terphenyl]-3,3''-dicarboxylate), did not lead to higher adsorption capacities as in our previous work,<sup>8</sup> but instead produced materials lacking step-shaped adsorption profiles. Finally, powder X-ray diffraction studies of both e-2-OH-Mg<sub>2</sub>(dobpdc) and *n*Pr-2-OH-Mg<sub>2</sub>(dobpdc) revealed a non-negligible *a-b* unit cell contraction upon CO<sub>2</sub> adsorption (-1.5% and -1.9%, respectively, Table S9), indicative of a favorable *a-b* interaction that is not evident with diamine-appended frameworks (-0.3% for e-2-Mg<sub>2</sub>(dobpdc)) (Table S9). Overall, these findings suggest that alcoholamine-appended frameworks likely exhibit *stabilizing* interactions in the *a-b* plane of the framework involving the interaction of two alcoholamines per molecule of CO<sub>2</sub> adsorbed.

## Mechanism of CO<sub>2</sub> Adsorption

### Metal effect

A key feature of ammonium carbamate chain formation in diamine-appended M<sub>2</sub>(dobpdc) frameworks is the influence of the metal center (Mg, Mn, Fe, Co, Ni, Zn) on the CO<sub>2</sub> adsorption step pressure, which arises due to the breaking of the M-N bond.<sup>7</sup> In contrast to our previous results with diamines,<sup>7,9</sup> only alcoholamine-appended variants of Mg<sub>2</sub>(dobpdc) were found to exhibit step-shaped adsorption profiles, as appending alcoholamines to the isostructural frameworks M<sub>2</sub>(dobpdc) (M = Mn, Co, Ni, Zn) produced adsorbents displaying non-cooperative adsorption profiles (SI, Section 8). This evidence lends significant

support for a cooperative process similar to that of the diamine-appended metal-organic frameworks,<sup>7</sup> whereby either a metal-

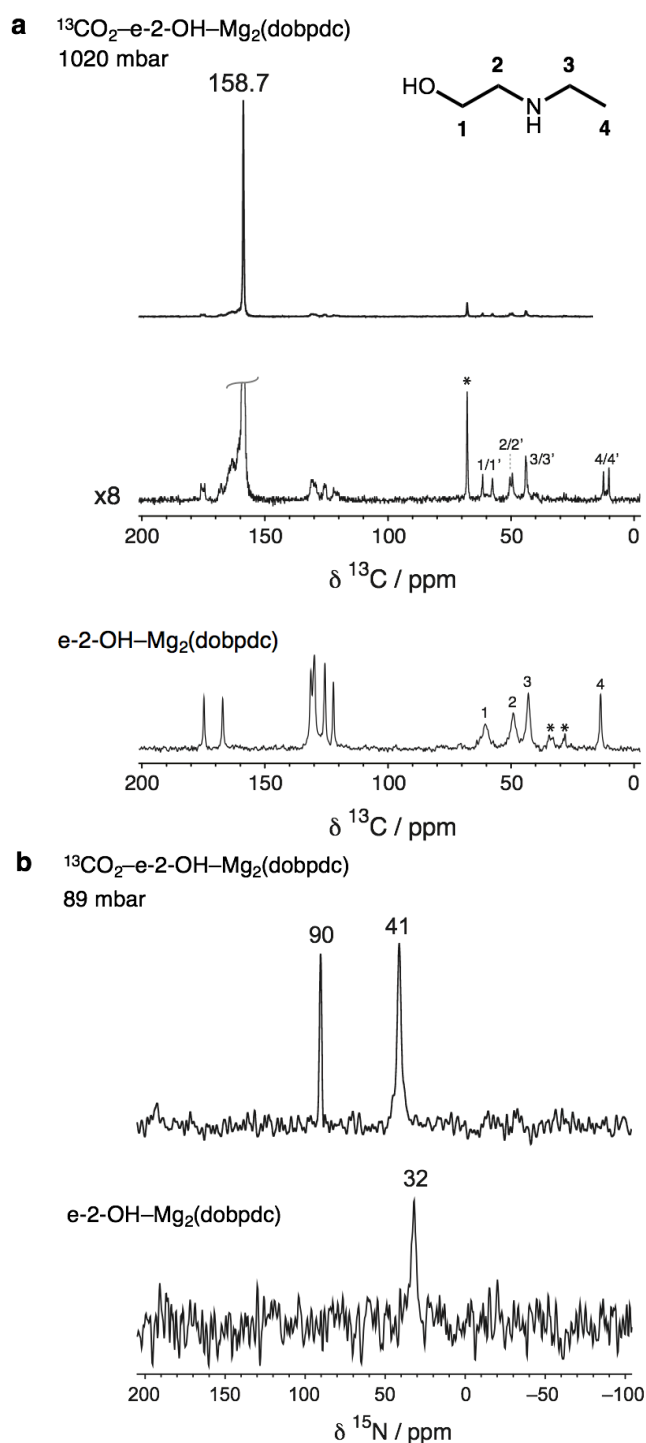


**Figure 4.** a) Activated (MAS rate = 17 kHz) and <sup>13</sup>CO<sub>2</sub>-dosed (MAS rate = 16 kHz) <sup>13</sup>C solid state magic angle spinning spectra of e-2-OH-Mg<sub>2</sub>(dobpdc). A small secondary <sup>13</sup>CO<sub>2</sub> resonance in e-2-OH-Mg<sub>2</sub>(dobpdc) at approximately 162 ppm likely arises from a minor side product from noncooperative chemisorption. b) Activated and <sup>13</sup>CO<sub>2</sub>-dosed <sup>15</sup>N solid state magic angle spinning spectra of e-2-OH-Mg<sub>2</sub>(dobpdc). Asterisks mark spinning side bands.

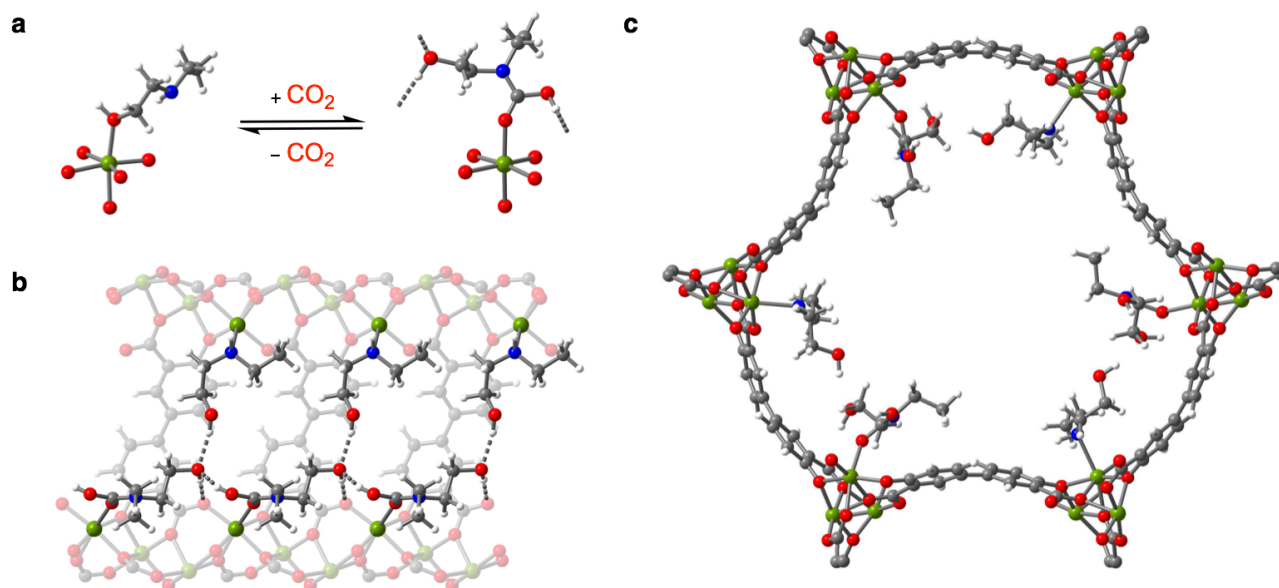


**Figure 5.** a) Structures of O-bound activated and CO<sub>2</sub>-inserted e-2-OH-Mg<sub>2</sub>(dobpdc). b) Predicted structure of CO<sub>2</sub>-inserted e-2-OH-Mg<sub>2</sub>(dobpdc), as viewed along the *c*-axis. c) View down the *c*-axis of the predicted structure of CO<sub>2</sub>-inserted e-2-OH-Mg<sub>2</sub>(dobpdc). All structures were calculated through DFT methods (SI, Section 17). Grey, red, blue, white, and green spheres represent C, O, N, H, and Mg atoms, respectively.

amine or metal-oxygen bond must be broken in order to adsorb CO<sub>2</sub> in a cooperative manner. Unfortunately, because large single crystals have to date only been accessible for the zinc framework, and because the alcoholamine-appended variants of Zn<sub>2</sub>(dobpdc) do not cooperatively adsorb CO<sub>2</sub>, it was not possible to obtain a single crystal X-ray diffraction structure of the CO<sub>2</sub>-inserted phases of any alcoholamine-appended frameworks.<sup>7,9</sup> While we were able to obtain the unit cell parameters for activated and CO<sub>2</sub>-dosed e-2-OH-Mg<sub>2</sub>(dobpdc) via powder X-ray diffraction, the structures proved to be too disordered to be solved. Therefore, it was necessary to turn to other characterization techniques to elucidate the CO<sub>2</sub> adsorption mechanism in alcoholamine-appended variants of Mg<sub>2</sub>(dobpdc).

#### Spectroscopic Evaluation

Solid-state magic angle spinning <sup>13</sup>C and <sup>15</sup>N NMR spectroscopy was utilized to examine local environments for e-2-OH-Mg<sub>2</sub>(dobpdc) upon adsorption of isotopically enriched <sup>13</sup>CO<sub>2</sub> (Figure 4). To serve as a point of reference, a <sup>13</sup>C and <sup>15</sup>N NMR spectrum of activated e-2-OH-Mg<sub>2</sub>(dobpdc) was first obtained. The resulting broad, low-intensity <sup>15</sup>N NMR resonance is consistent with our DFT predictions of dynamic O/N binding (Figure S190). Upon dosing the sample with <sup>13</sup>CO<sub>2</sub>, a dominant <sup>13</sup>C resonance was observed at 158.7 ppm. This chemical shift is smaller compared to those of the ammonium carbamates formed in diamine-appended frameworks<sup>7,9,12,13,24</sup> and is more similar to the previously reported shifts for the carbonyl carbons of carbamic acids and ammonium alkylcarbonates.<sup>12,13,16,17,24</sup> In the <sup>13</sup>C NMR spectrum of <sup>13</sup>CO<sub>2</sub>-dosed e-2-OH-Mg<sub>2</sub>(dobpdc), splitting of the alcoholamine <sup>13</sup>C resonances was immediately apparent, consistent with the observed adsorption of CO<sub>2</sub> at only half of the alcoholamine sites in alcoholamine-appended variants of Mg<sub>2</sub>(dobpdc). In addition, <sup>13</sup>C-<sup>1</sup>H NMR correlation measurements indicate the presence of carbamic acid or ammonium <sup>1</sup>H (11.4 ppm) strongly interacting with the carbonyl carbon of the CO<sub>2</sub>-

adsorbed product (SI, Figure S186). This <sup>1</sup>H chemical shift is similar to those previously measured for carbamic acids and is lower than those for secondary diamines forming ammonium carbamates,<sup>24</sup> thus suggesting that this new product is most likely a carbamic acid.

In the <sup>15</sup>N NMR spectrum of <sup>13</sup>CO<sub>2</sub>-dosed e-2-OH-Mg<sub>2</sub>(dobpdc) (Figure 4a), two distinct resonances at larger chemical shifts relative to the activated alcoholamine nitrogen shifts were observed. The resonance at approximately 90 ppm is assigned to an amine that has reacted with CO<sub>2</sub> and is higher than any corresponding chemical shift for diamine-appended metal-organic frameworks.<sup>24</sup> Importantly the observation of this resonance confirms that CO<sub>2</sub> reacts at nitrogen, rather than at oxygen (SI, Section 18). The resonance at approximately 41 ppm likely corresponds to a free alcoholamine participating in hydrogen bonding due to the higher chemical shift compared to that observed for the activated alcoholamine-appended framework. The similarity in resonance intensities between the two sets of alcoholamine resonances in the <sup>13</sup>C NMR spectrum and the two resonances in the <sup>15</sup>N spectrum indicates that the two distinct alcoholamine environments are in equal proportion, further supporting the participation of the free alcoholamine in hydrogen bonding interactions with the CO<sub>2</sub>-adsorbed product. These experiments were repeated for *i*Pr-2-OH-Mg<sub>2</sub>(dobpdc) and very similar results were observed (SI, Section 16), which suggests that alcoholamine-appended variants of Mg<sub>2</sub>(dobpdc) follow the same general CO<sub>2</sub> adsorption mechanism.

#### DFT Calculations

Motivated by our previous experimental<sup>7,9,10,24</sup> and computational<sup>11,23</sup> studies of the mechanisms of CO<sub>2</sub> adsorption in diamine-appended metal-organic frameworks, we investigated five potential mechanisms for cooperative CO<sub>2</sub> adsorption in e-2-OH-Mg<sub>2</sub>(dobpdc) by van der Waals (vdW)-corrected Density Functional Theory (DFT) calculations (SI, section 18). This

structural analysis led to a promising candidate structure for CO<sub>2</sub> adsorption in e-2-OH-Mg<sub>2</sub>(dobpdc) involving the unprecedented formation of carbamic acid chains (Table 1, Figure 5). The carbamic acid chain structure (Mechanism A, Figure 5) shows the best agreement between the various calculated and experimental parameters (Table 1, Table S11, SI section 18).

**Table 1.** Computed free energies (*E*), CO<sub>2</sub> binding energies (*E<sub>B</sub>*), lattice parameters and chemical shifts of Mechanism A of CO<sub>2</sub> insertion in e-2-OH-Mg<sub>2</sub>(dobpdc). The binding energy was calculated using O-bound e-2-OH-Mg<sub>2</sub>(dobpdc) as a starting reference, as we have also found this to be the most energetically favorable structure for almost all alcoholamines and within calculational error for O- vs. N-bound e-2-OH-Mg<sub>2</sub>(dobpdc) (Table S10). Errors are indicated in parentheses.

	Experimental	Mechanism A
<i>E<sub>B</sub></i> (kJ/mol)	-81(4)	-79
<i>a</i> (Å)	21.255(1)	21.299
<i>c</i> (Å)	6.875(4)	7.053
δ <sup>13</sup> C (C=O) (ppm)	158.7(1)	158.5
δ <sup>15</sup> N (ppm)	90(1) (inserted N) 41(1) (free N)	102.4 (inserted N) 38.7 (free N)

The proposed mechanism is similar to the ammonium carbamate chain mechanism observed experimentally in many diamine-appended frameworks<sup>7,10</sup> but without proton transfer to a neighboring amine, leading to a two-fold hydrogen bond-stabilized carbamic acid chain. Hydrogen bond donation occurs from the carbamic acid to the neighboring O of the terminal alcohol, which itself donates a hydrogen bond to the non-bridging carboxylate oxygen atom of the ligand. This complex is further stabilized via O-H hydrogen bond donation from the neighboring alcoholamine in the *a-b* plane of the framework. The extensive hydrogen bonding network likely accounts for the energetic stability of this structure despite the documented instability of carbamic acids.<sup>19-22</sup> Furthermore, this mechanism captures the experimentally observed capacity of one CO<sub>2</sub> per two alcoholamines and the *a-b* unit cell contraction observed by powder X-ray diffraction (Table S9). Although we considered the possibility of the amine of the free alcoholamine to act as a hydrogen bond donor, we found this structure to be less energetically favorable (Figure S194).

#### Expanding Cooperativity to Alkoxyalkylamine-Functionalized Mg<sub>2</sub>(dobpdc) Variants.

Consistent with our general mechanistic hypothesis, we have preliminarily found that primary alkoxyalkylamine-functionalized Mg<sub>2</sub>(dobpdc) variants also display step-shaped adsorption profiles (Figure 6). In this case, the mechanism is predicted to be similar to that with alcoholamine-appended frameworks but with additional proton transfer from the carbamic acid to a neighboring, uninserted amine in the *a-b* plane to form

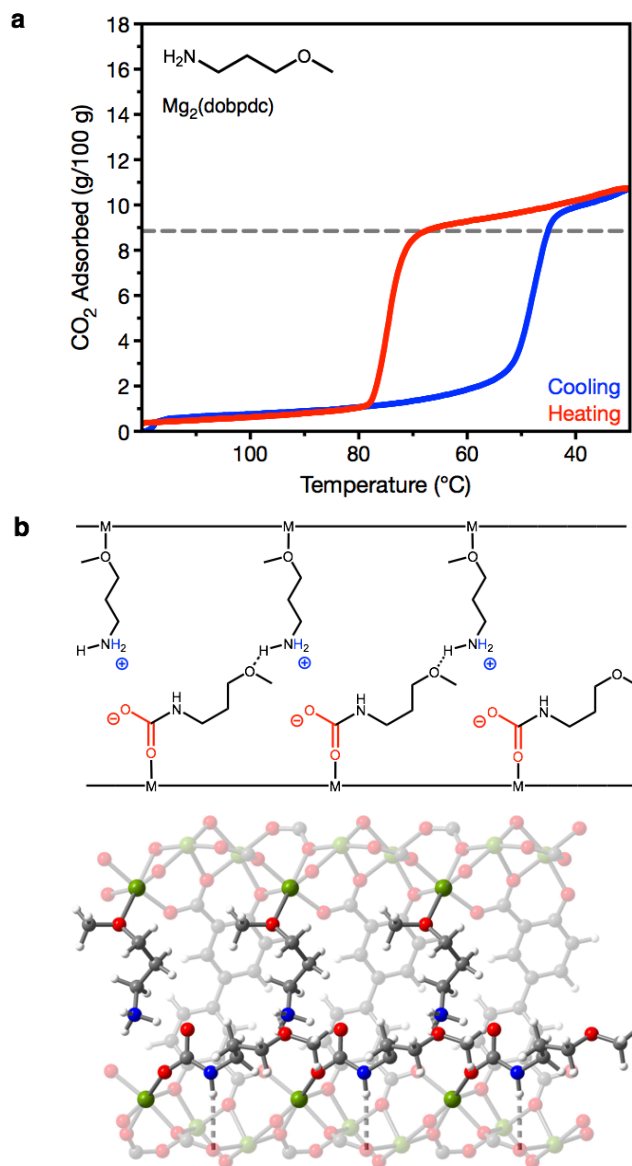


**Figure 6.** a) Pure CO<sub>2</sub> adsorption (blue) and desorption (red) isobars at atmospheric pressure for 3-O-m-Mg<sub>2</sub>(dobpdc), as measured by thermogravimetric analysis. The grey dash indicates 1 CO<sub>2</sub> per two molecules of 3-O-m. b) Predicted structure of CO<sub>2</sub>-inserted 3-O-m-Mg<sub>2</sub>(dobpdc), as viewed along the *c*-axis. All structures were calculated through DFT methods (SI, Section 17). Grey, red, blue, white, and green spheres represent C, O, N, H, and Mg atoms, respectively.

an ammonium carbamate. As our experimental isobaric and isothermal data, <sup>1</sup>H NMR and <sup>13</sup>C NMR, and DFT calculations reveal that this adsorption mechanism is likely structurally similar to that of e-2-OH-Mg<sub>2</sub>(dobpdc), we leave this discussion to the SI. Based on these initial findings, it appears that the mechanism of CO<sub>2</sub> adsorption may be functionality dependent, wherein switching alcohols for ethers lowers the stability of carbamic acid in favor of ammonium carbamate.

## IV. Conclusion

We have discovered the first experimentally verified cooperative mechanism for CO<sub>2</sub> chemisorption that does not

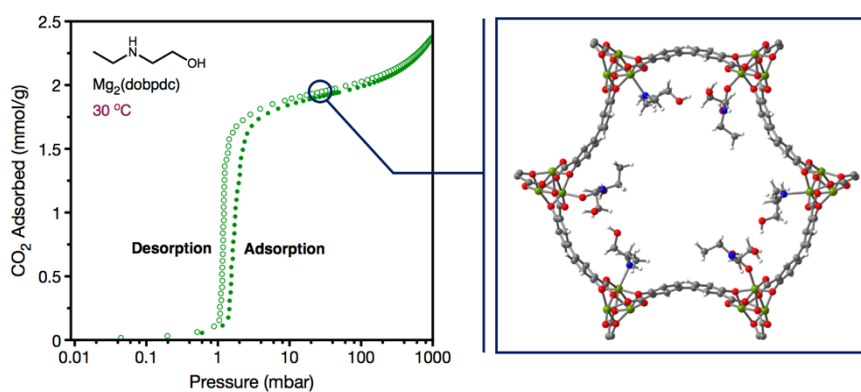
involve diamines, exhibited in a variety of structurally diverse alcoholamine- and alkoxyalkylamine-functionalized variants of the metal–organic framework Mg<sub>2</sub>(dobpdc). Namely, secondary alcoholamines with moderately large alkyl substituents, as well as primary alkoxyalkylamines, demonstrate selective, step-shaped adsorption and desorption of CO<sub>2</sub> in Mg<sub>2</sub>(dobpdc). Computational structural studies, solid state NMR spectroscopy, and other experimental evidences indicate that the observed adsorption capacity of 1 CO<sub>2</sub> per 2 alcoholamines or alkoxyalkylamines arises due to hydrogen-bonding chain structures that are stabilized by additional interactions in the *a-b* plane of the framework. This new adsorption mechanism greatly increases the scope of functionalized materials that undergo cooperative CO<sub>2</sub> adsorption and paves the way for the discovery of new materials and mechanisms for carbon capture applications.

## Acknowledgements

We thank the National Institute of General Medical Sciences of the National Institutes of Health for a postdoctoral fellowship for P.J.M. (F32GM120799). The content is solely the responsibility of the authors and does not necessarily represent the official views of the National Institutes of Health. We thank the Philomathia Foundation for fellowships for A.C.F. and C. M. M. We thank the SURF Rose Hills for support of L.B.P.-Z. through a summer research fellowship. Crystallographic and solid-state NMR studies were supported through the Center for Gas Separations Relevant to Clean Energy Technologies, an Energy Frontier Research Center funded by the U.S. Department of Energy (DoE), Office of Science, Office of Basic Energy Sciences, under Award DE-SC0001015. This work utilized the resources of the Advanced Photon Source, DoE Office of Science User Facility operated for the DoE Office of Science by Argonne National Laboratory under Contract No. DE-AC02-06CH11357. We thank Henry Jiang and Julia Oktawiec (UC Berkeley) for experimental assistance with powder X-ray diffraction and for preliminary infrared spectroscopy studies.

**Keywords:** Carbon Capture • Density Functional Calculations • Inorganic Chemistry Materials Science: General • Metal-Organic Frameworks • NMR Spectroscopy

- [1] ESRL Global Monitoring Division - Global Greenhouse Gas Reference Network, can be found under [www.esrl.noaa.gov/gmd/ccgg/trends/](http://www.esrl.noaa.gov/gmd/ccgg/trends/), **2018**.
- [2] Inventory of U.S. Greenhouse Gas Emissions and Sinks: 1990-2016 – Executive Summary; U.S. EPA., 2018.
- [3] R. S. Haszeldine, *Science* **2009**, 325 (5948), 1647–1652.
- [4] S. J. J. Titinchi, M. Piet, H. S. Abbo, O. Bolland, Schwioger, W. *Energy Procedia* **2014**, 63, 8153–8160.
- [5] S. Solomon, G. Plattner, R. Knutti, P. Friedlingstein, *P. Natl. Acad. Sci. USA* **2009**, 106 (6), 1704–1709.
- [6] W. Knorr, *Geophys. Res. Lett.* **2009**, 36.
- [7] T. M. McDonald, J. A. Mason, X. Kong, E. D. Bloch, D. Gygi, A. Dani, V. Crocella, F. Giordanino, S. O. Odoh, W. S. Drisdell, B. Vlasisavljevich, A. L. Dzubak, R. Poloni, S. K. Schnell, N. Planas, K. Lee, T. Pascal, L. F. Wan, D. Prendergast, J. B. Neaton, B. Smit, J. B. Kortright, L. Gagliardi, S. Bordiga, J. A. Reimer, J. R. Long, *Nature* **2015**, 519 (7543), 303–308.
- [8] P. J. Milner, J. D. Martell, R. L. Siegelman, D. Gygi, S. C. Weston, J. R. Long, *Chem. Sci.* **2018**, 9, 160.
- [9] P. J. Milner, R. L. Siegelman, A. C. Forse, M. I. Gonzalez, T. Runcevski, J. D. Martell, J. A. Reimer, J. R. Long, *J. Am. Chem. Soc.* **2017**, 139, 13541–13553.
- [10] R. L. Siegelman, T. M. McDonald, M. I. Gonzalez, J. D. Martell, P. J. Milner, J. A. Mason, A. H. Berger, A. S. Bhowan, J. R. Long, *J. Am. Chem. Soc.* **2017**, 139, 10526.
- [11] J. Lee, R. Siegelman, L. Maserati, T. Rangel, B. A. Helms, J. R. Long, J. B. Neaton, *Chem. Sci.*, **2018**, 9, 5197.
- [12] R. W. Flaig, T. M. Popp, A. M. Fracoli, E. A. Kapustin, M. J. Kalmutzki, R. M. Altamimi, F. Fathieh, J. A. Reimer, O. M. Yaghi, *J. Am. Chem. Soc.* **2017**, 139 (35), 12125–12128.
- [13] C. Chen, D. Shimon, J. L. Lee, S. A. Didas, A. K. Mehta, S. Carsten, C. W. Jones, S. E. Hayes, *Environ. Sci. Technol.*, **2017**, 51 (11), 6553–6559.
- [14] B. Lv, B. Guo, Z. Zhou, G. Jing, *Environ. Sci. Technol.* **2015**, 49 (17), 10728–10735.
- [15] B. R. Strazisar, R. R. Anderson, C. M. White, *Energ. Fuel* **2003**, 17, 1034–1039.
- [16] L. Mafra, T. Cendak, S. Schneider, P. V. Wiper, J. Pires, J. R. B. Gomes, M. L. Pinto, *J. Am. Chem. Soc.* **2017**, 139 (1), 389–408.
- [17] M. L. Pinto, L. Mafra, J. M. Guil, J. Pires, J. Rocha, *Chem. Mater.* **2011**, 23, 1387–1395.
- [18] Y. Cheon, Y. M. Jung, J. Lee, H. Kim, J. Im, M. Cheong, H. S. Kim, H. S. Park, *ChemPhysChem* **2012**, 13, 3365–3369.
- [19] A. Danon, P. C. Stair, E. Weitz, *J. Phys. Chem. C* **2011**, 115, 11540.
- [20] J.-B. Bossa, F. Borget, F. Duvernay, P. Theule, T. Chiavassa, *J. Phys. Chem. A* **2008**, 112, 5113.
- [21] K. Masuda, Y. Ito, M. Horiguchi, H. Fujita, *Tetrahedron* **2005**, 61, 213.
- [22] R. K. Khanna, M. H. Moore, *Spectrochim. Acta, Part A* **1999**, 55, 961.
- [23] B. Vlasisavljevich, S. O. Odoh, S. Schnell, A. L. Dzubak, K. Lee, N. Planas, J. B. Neaton, L. Gagliardi, B. Smit, *Chem. Sci.* **2015**, 6, 5177.
- [24] A. C. Forse, P. J. Milner, J. Lee, H. N. Redfeam, J. Oktawiec, R. L. Siegelman, J. D. Martell, B. Dinakar, L. B. Porter-Zasada, M. I. Gonzalez, J. B. Neaton, J. R. Long, J. A. Reimer. In Preparation.



V. Y. Mao, P. J. Milner, J. Lee, A. C. Forse, H. Jiang, E. Kim, R. L. Siegelman, C. M. McGuirk, L. Porter-Zasada, J. B. Neaton, J. A. Reimer, and J. R. Long \*

**Cooperative Carbon Dioxide Capture in Alcoholamine- and Alkoxyalkylamine-Functionalized Metal–Organic Frameworks**

The first documented cooperative CO<sub>2</sub> chemisorption mechanism without the usage of diamine is described. Step-shaped adsorption is observed and characterized in a variety of structurally-diverse alcoholamine and alkoxyalkylamine-functionalized metal-organic frameworks. It is found that carbamic acid or ammonium carbamate formation can result, and that the formation of hydrogen-bonded chain structures likely leads to the observed adsorption steps.